Macromolecules
ARTICLE

Macromolecules **2009**, *42*, 6733–6740 **6733**
DOI: 10.1021/ma901209x

Single Polyelectrolyte Layers Adsorbed at High Salt Conditions: Polyelectrolyte Brush Domains Coexisting with Flatly Adsorbed Chains

Stephan Block and Christiane A. Helm*

Institut für Physik, Ernst-Moritz-Arndt Universität, Felix-Hausdorff-Str. 6, D-17487 Greifswald, Germany

Received June 5, 2009; Revised Manuscript Received July 10, 2009

ABSTRACT: AFM is used to measure the surface forces and to image sodium poly(styrenesulfonate) (PSS) layers physisorbed from 1 M NaCl solution on different length scales within one experiment. Domains of PSS brushes coexist with flatly adsorbed PSS. For degree of polymerization $N = 380$, the brush area fraction is 6%. With increasing degree of polymerization, brush area fraction and domain size increase, whereby the domain radii vary between 50 nm and 1.5 μm. Lateral homogeneous brush layers are found for a degree of polymerization exceeding 1100. The colloidal probe technique reveals that the surface forces are a superposition of steric and electrostatic forces; their respective contribution is determined by the brush area fraction. A comparison with literature demonstrates that adsorbed PSS brushes show the same scaling behavior as end-grafted PSS brushes. We develop a model for the adsorption of polyelectrolytes in which not the whole chain but only a fraction of the monomers adsorbs onto the surface. Thereby, we show that partial adsorption can lead to stable conformations and calculate scaling laws for the fraction of adsorbed monomers and the distance between the chains dangling into solution.

Introduction

Adsorbed polyelectrolytes are used in a multitude of traditional applications (e.g., as wet and dry strength additives) but also in basic research in connection with material and the life sciences.[1−5] Because of their ionizable groups (incorporated within the monomeric units), polyelectrolytes can be used as flocculating or dispersing agent in industrial applications.[6,7] Furthermore, the electrostatic monomer−monomer repulsion can be used to stabilize colloidal suspensions, a mechanism which is very efficient if end-grafted polyelectrolyte brushes are used.[8]

However, a controlled end-grafting of polyelectrolyte brushes requires a much more complex process than polyelectrolyte adsorption. In previous work we showed that linear polyelectrolytes physisorbed from 1 M NaCl solution exhibit a nonflat conformation[9,10] very similar to that of polyelectrolyte brushes (i.e., the thickness of the physisorbed layer scales like a salted polyelectrolyte brush: on decrease of the surrounding salt concentration it can reach up to 1/3 of the contour length). Surface forces between such layers obtained by colloidal probe technique were described with the theory of Alexander and de Gennes[11] for anchored neutral polymers. This was done since this theory is experimentally indistinguishable from the theories of Milner, Witten, Cates[10,12] (for polymer brushes), and Biesheuvel[13,14] (for polyelectrolyte brushes) and gives the simplest force law (i.e., the simplest formula). This behavior differs very much from polyelectrolytes adsorbed from salt-free solution, which build a flat adsorption layer and show an electrostatic repulsion.[15−18] (The same flat layer is found at the bottom of the brush formed by adsorption at 1 M NaCl. The flat layer can be characterized if an AFM tip instead of a colloidal probe is used.[10])

Therefore, by addition of 1 M NaCl to the adsorption solution we are able to increase the range and strength of the repulsive force created by the polyelectrolyte layer and hence to create a more effective colloidal stabilization. However, the influence of the chain length on the repulsive force remains unknown. (For a more detailed review about theoretical and experimental aspects of polyelectrolyte−surface mediated interactions, please refer to the work of Podgornik et al.[19])

We will describe the surface properties of linear sodium poly(styrenesulfonate) (PSS) layers formed by adsorption from 1 M NaCl solution (at 30 °C, 1 h adsorption time) onto silanized silica substrates (the silane has a positively charged end-group). We show that in general PSS layers are composed by a two-phase system: a PSS brush phase that coexists with flatly adsorbed PSS. Using colloidal probe tapping mode (CPTM[9]), we are able to image the domains of the PSS brush phase and therefore to study the spatial properties of these domains. By connecting the measurements of CPTM with force measurements using colloidal probe technique (CPT[20,21]), we will completely characterize the properties of the brush phase and we will derive the scaling laws for brush thickness L, average chain distance s, and brush area fraction A with respect to the degree of polymerization N. Thereby, we are able to set the range and strength of the steric repulsion by choosing an appropriate value of N.

Materials and Methods

All solutions are created with ultrapure water using a Milli-Q device (Millipore, Billerica, MA). Sodium chloride (NaCl, p.a. grade) was obtained from Merck (Darmstadt, Germany) and 3-aminopropyldimethylethoxysilane from ABCR (Karlsruhe, Germany). Sodium poly(styrenesulfonate) (PSS) with monomer count ranging from $N = 380$ (contour length $L_C = 95$ nm) to 1800 ($L_C = 450$ nm) was purchased from Polymer Standard Service (Mainz, Germany) in the following batches: pss13030 (77 kDa, $N = 380$, PDI < 1.1), pss14061 (123 kDa, $N = 600$, PDI < 1.2), pss26058 (168 kDa, $N = 840$, PDI < 1.2), and pss200203 (350 kDa, $N = 1800$, PDI < 1.2). PSS with an average mass of 1.4 MDa ($N = 6800$, $L_C = 1700$ nm, PDI < 1.2) was a generous gift of BASF (Ludwigshafen, Germany).

All chemicals are used without further purification. The PSS deposition solution is prepared by solving 1 M NaCl and 3 mM PSS (with respect to the monomer concentration) in Milli-Q water.

Colloidal probes (CP) are created by gluing silica spheres (from Bangs Laboratories, Fishers, IN; radius $R = 3$ μm, determined using an optical microscope) with UV-curable epoxy (NOA68,

*To whom correspondence should be addressed.

Published on Web 08/12/2009

Norland Adhesives, Cranbury, NJ) onto the following cantilevers: for colloidal probe tapping mode (CPTM[9]) cantilevers NP-0 (spring constant $k = 0.58$ N/m) from Veeco (Dourdan, France); for Colloidal Probe Technique (CPT[20,21]) cantilevers CSC12 (spring constant $k = 0.005-0.03$ N/m) from MicroMasch (Tallin, Estonia).

Surface Preparation. Microscope slides (Roth, Karlsruhe, Germany) are used as silica surfaces. They are cleaned according to the RCA standard and freshly used. CPs are cleaned with argon plasma at 35 W for 2 min (Harrick Scientific, NY) and are used immediately (if they are intended for CPTM or asymmetric force measurements). The surfaces (intended for PSS adsorption) are positively charged by silanization (1 day in argon−silane atmosphere, direct use after silanization) and coated with PSS by physisorption from 1 M NaCl solution for 1 h at 30 °C. After adsorption the surfaces are directly transferred (i.e., without drying) into the fluid cell of our commercial DI Multimode AFM with Nanoscope IIIa Controller (Santa Barbara, CA).

Force Measurements. The force measurements are performed after PSS adsorption in NaCl solutions (free of PSS) of different ionic strengths: starting at 0.1 M, then diluting down to 1 mM, and enriching again to 0.1 M. Force curves are recorded not later than 5 min after change of the solution. We perform symmetric measurements (both surfaces covered with PSS) as well as asymmetric measurements (one PSS covered surface against a bare silica CP or a silicon tip). During one experiment we record at least 200 force curves for each salt concentration at different positions on the surface, with one approach/separation cycle per 5 s. Shown are only the averaged force curves. After the measurement spring constants are determined using the methods of Butt, Sader, and Cleveland.[22−24] All in all, more than 55 000 force curves were recorded.

Imaging. The morphology of the PSS layers is measured using AFM colloidal probe tapping mode (CPTM) in PSS-free NaCl solutions of different ionic strengths (between 1 M and 1 mM NaCl as indicated), as described in ref 9. In this study 512 × 512 pixels are recorded per image, and the *z*-limit of the piezo scanner was set to 500 nm, in order to increase the height resolution of the AFM. Directly after preparation (of the CP) CPTM images with a coarse lateral resolution (curvature radius = CP radius $R = 3\,\mu$m) are obtained. Imaging with a finer lateral resolution without changing the CP is possible as follows: at high surrounding salt concentrations $I > 0.1$ M NaCl, the electrostatic repulsion between negatively charged CP and PSS chains is low, and therefore it is possible to attach a small fraction of PSS chains onto the CP by van der Waals attraction. Afterward, it is possible to determine the effective curvature radius of the "PSS tip" by using a self-imaging artifact, like Nioprobe from Aurora NanoDevices Inc. (Nanaimo, Canada) or TGT01 from MicroMasch (Tallin, Estonia); cf. Figure S1 in the Supporting Information.

Image Processing. Images obtained with the AFM are stored in raw data format, i.e., in the absence of any automated filtering or image processing by the AFM software. Afterward, the images are processed using the Nanoscope 5 software (which is delivered with our commercial DI Multimode AFM) as follows: For larger images (scan area $> 1 \times 1\,\mu$m) the spherical distortion introduced by the piezo scanner is removed by fitting a spherical plane (of second order) into the data and by subtracting the fitted spherical plane from the data. For smaller images this correction is skipped, as no distortion was noticeable.

Reproducibility. All measurements (CPT and imaging) are repeated at least twice with freshly prepared surfaces.

Morphology of the Adsorbed PSS Layers

The morphology of the PSS layers (physisorbed from 1 M NaCl solution) is investigated using CPTM as described in ref 9. Here, the use of a bare colloidal probe (CP) instead of a sharp tip increases the contact area and hence the interaction between the cantilever and the PSS chains protruding into solution. Figure 1 shows the PSS layer morphology ($N = 380 \ldots 6800$) as measured in an aqueous solution containing $I = 1$ mM NaCl. For $N \geq 1800$ we see a homogenously adsorbed PSS layer, and in ref 9 we showed that the whole layer is a PSS brush as its swelling/shrinking behavior (quantitatively) equals that of PSS brush if I is changed. However, as the degree of polymerization is decreased, the layer starts to exhibit holes (Figure 1b, $N = 840$, dotted circles), and eventually islands are observed (Figure 1c, $N = 600$, dash-dotted circles), whose height exceeds 10 nm. Furthermore, the height depends reversibly on I (cf. Figure 2a−c), a behavior characteristic for polyelectrolyte brushes. Using these swelling/shrinking experiments, we infer that the islands are domains formed by adsorbed PSS brushes.

However, for the shortest PSS ($N = 380$) the layer appears homogeneous again (Figure 1d), but homogeneous refers to the length scale of the CP (radius $R \approx 3\,\mu$m). Fortunately, at high I we are able to attach a small fraction of PSS onto the CP leading to a "tip" (curvature radius ≈ 100 nm, cf. Supporting Information), which acts like a "sharp tip". Hence, we are able to investigate the surface morphology of the PSS layers on two different length scales (approximately 100 nm vs 3 μm) within one experiment at the same position. Applied to $N = 380$, we find that the layer appears homogeneous only on the coarse length scale (Figure 2d, $R \approx 3\,\mu$m, same image as Figure 1d but the *z*-scale is reduced to increase the contrast), whereas small islands are visible on the fine length scale (Figure 2e,f) which we again attribute to PSS brush domains.

Surprisingly the images show that there are two distinct PSS phases: In the first phase the PSS chains are adsorbed flatly, i.e., in a 2D conformation,[25] whereas the second phase consists of chains that are adsorbed in a coiled (3D) conformation and which show a behavior similar to polyelectrolyte brushes (i.e., a change of surrounding salt concentration I leads to reversible swelling/shrinking on 10−100 nm scale; cf. Figure 2c). Obviously, the area ratio of these two phases strongly depends on the degree of polymerization N; i.e., the area fraction of the brush phase scales with $N^{2.5}$ and reaches 100% around $N = 1100$ (see inset of Figure 4).

From Figure 2c,f one can infer that the average domain radius is 45 nm ($N = 380$) and 1.5 μm ($N = 600$). This shows that we are able to vary the size of the domains and hence the length scale of these "patches" over 2 orders of magnitude by choosing an appropriate N.

Furthermore, these patches affect surface properties like the rms-roughness σ (which depends on N and I). Generally, as swelling/shrinking effects of the brush phase are only resolved by the CP, we notice no dependence on I if a tip ($R \approx 100$ nm) is used for imaging. Actually, if a tip is used for $N \geq 600$, the images show only the PSS layer at the bottom of the brush, a behavior which we attribute to tip penetration of the brush phase.[10] These images exhibit a rms roughness σ around 6 Å, which is independent of I. For $N = 380$ the brush phase can be imaged by the tip, and here σ is increased to 15 Å (i.e., the tip no longer penetrates; cf. Figure 2f). Using a CP for imaging, we notice a dependence of σ on I for $N \leq 600$, which is related to swelling/shrinking of the brush phase. For $N = 380$, σ increases from 7 Å ($I = 0.1$ M) to 10 Å ($I = 1$ mM) and for $N = 600$ from 12 Å ($I = 0.1$ M) to 25 Å ($I = 1$ mM). This increase is significant as the statistical error in the determination of σ is less than 1 Å. For larger chains ($N \geq 840$) σ becomes independent of I again, as the CP is not able to penetrate through the brush phase (area fraction > 50%): for $N = 840$ the rms roughness is about 20 Å, which reduces to 9 Å for $N = 1800$ and 6800. Hence, the rms roughness is relatively small ($\sigma < 10$ Å) if only one phase is adsorbed to the surface (i.e., $A \approx 0$ or $A \approx 1$), whereas it reaches significantly higher values if the surface is laterally structured ($A \approx 50\%$).

However, we found[10] that the flatly adsorbed PSS chains create an electrostatic force (due to charge overcompensation[25]),

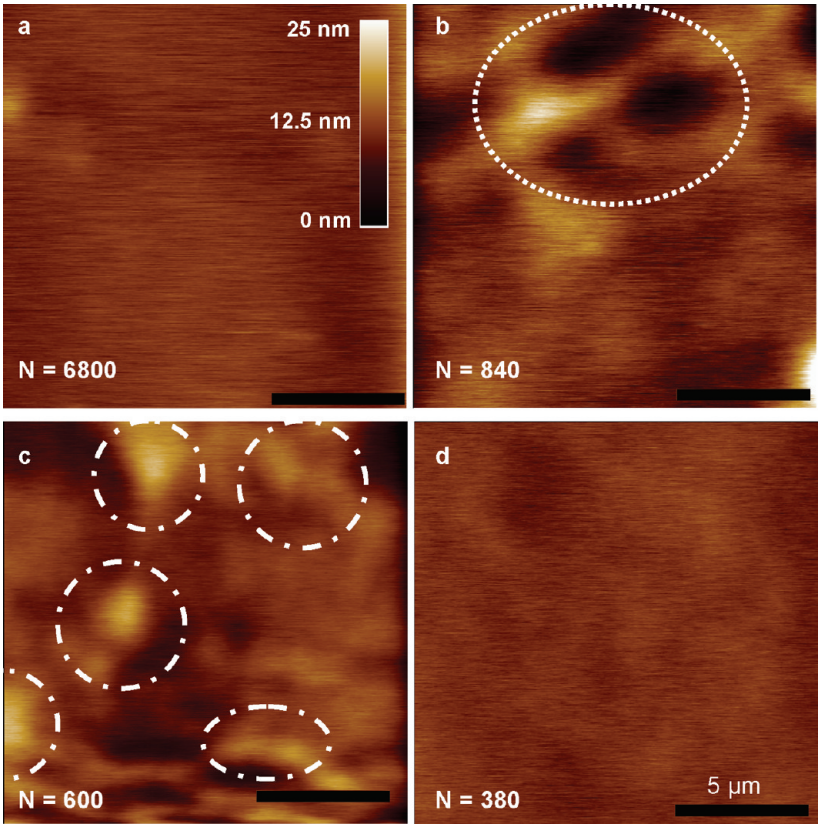

Figure 1. Colloidal probe tapping mode (CPTM) images of PSS layers (with degree of polymerization as indicated), adsorbed from 1 M NaCl solution onto silanized silica, measured at $I = 1$ mM (scale bar = 5 μm, z-range = 25 nm). For long PSS (a, $N = 1800, 6800$) the layer appears homogeneous, whereas a decrease in N leads to holes (b, dotted circles) and islands (c, dash-dotted circles). The islands are brush domains, a fact which was proven by swelling experiments (cf. Figure 2a–c). For $N = 380$ (d) the layer appears homogeneously again on the length scale of the colloidal probe (CP, radius $R \approx 3$ μm).

whereas the brush phase shows only a steric force. Hence, we conclude that in general the force (acting between two PSS covered surfaces) will be a superposition of an electrostatic and a steric force whose respective contribution depends on the area fraction A of the brush phase.

Force Curves

The structure of the composed force profile for the asymmetric case (a bare silica CP interacts with a PSS covered surface) and the symmetric case (both interacting surfaces are covered by PSS) were derived and validated in ref 26. From the definition of the brush phase area fraction A we infer that in the asymmetric case the fraction A of the unit area creates an asymmetric steric force whereas the fraction $(1 - A)$ shows an electrostatic force. Thus, the composed force profile has the form

$$F(D) = (1 - A)F_{\mathrm{DL,\,asymm}}(D) + AF_{\mathrm{AdG,\,asymm}}(D) \qquad (1a)$$

with $F_{\mathrm{DL,asymm}}$ denoting the asymmetric electrostatic force (acting between a flatly adsorbed PSS layer and a silica surface) and $F_{\mathrm{AdG,asymm}}$ the asymmetric steric force profile (see next paragraph and eq 3b). Furthermore, in the symmetric case the electrostatic, asymmetric steric, and symmetric steric forces contribute with fractions $(1 - A)^2$, $2A(1 - A)$, and A^2, respectively, to the composed force profile, leading to

$$F(D) = (1 - A)^2 F_{\mathrm{DL,\,symm}}(D) + 2A(1 - A)F_{\mathrm{AdG,\,asymm}}(D) + A^2 F_{\mathrm{AdG,\,symm}}(D) \qquad (1b)$$

with $F_{\mathrm{DL,symm}}$ denoting the symmetric electrostatic force (acting between two flatly adsorbed PSS layers) and $F_{\mathrm{AdG,symm}}$ the symmetric steric force profile (cf. eq 3a). This follows from the fact that in the symmetric case both surfaces are laterally structured and inhomogeneously covered by the brush phase.

In ref 27 it is shown that for monovalent salts, at surface separations D larger than the Debye length κ^{-1} ($= 0.304\ \mathrm{nm}/\sqrt{I}$) and for surface potentials $\psi_{0,1/2} < 25$ mV the electrostatic repulsion F_{DL} can be well approximated by

$$\frac{F_{\mathrm{DL}}(D)}{2\pi R} = 0.0482\sqrt{I}\,\tanh\left[\frac{\Psi_{0,1}}{103\ \mathrm{mV}}\right]\tanh\left[\frac{\Psi_{0,2}}{103\ \mathrm{mV}}\right]\mathrm{e}^{-\kappa D} \qquad (2)$$

where $\psi_{0,1/2}$ denotes the respective surface potential at infinite surface separation D. Hence, setting $\psi_{0,1} = \psi_{0,\mathrm{PSS}}$ and $\psi_{0,2} = \psi_{0,\mathrm{silica}}$ in eq 2 leads to $F_{\mathrm{DL,asymm}}$, whereas setting $\psi_{0,1} = \psi_{0,2} = \psi_{0,\mathrm{PSS}}$ results in $F_{\mathrm{DL,symm}}$.

Furthermore, in ref 10 (with $A = 100\%$) we have shown that the steric forces in eq 1 can be completely described using the theory of Alexander and de Gennes (called AdG theory below[11]). This theory was originally derived to describe the steric force acting between two non-interpenetrating end-grafted neutral polymer-brushes and leads to an interaction energy per unit area of two brushes (of thickness L and grafting density $\Gamma = s^{-2}$)[10,28]

$$\frac{F_{\mathrm{AdG,\,symm}}(D)}{2\pi R} = \frac{8k_{\mathrm{B}}TL}{35s^3}\left[7\left(\frac{2L}{D}\right)^{5/4} + 5\left(\frac{D}{2L}\right)^{7/4} - 12\right] \quad \text{for } D < 2L \qquad (3a)$$

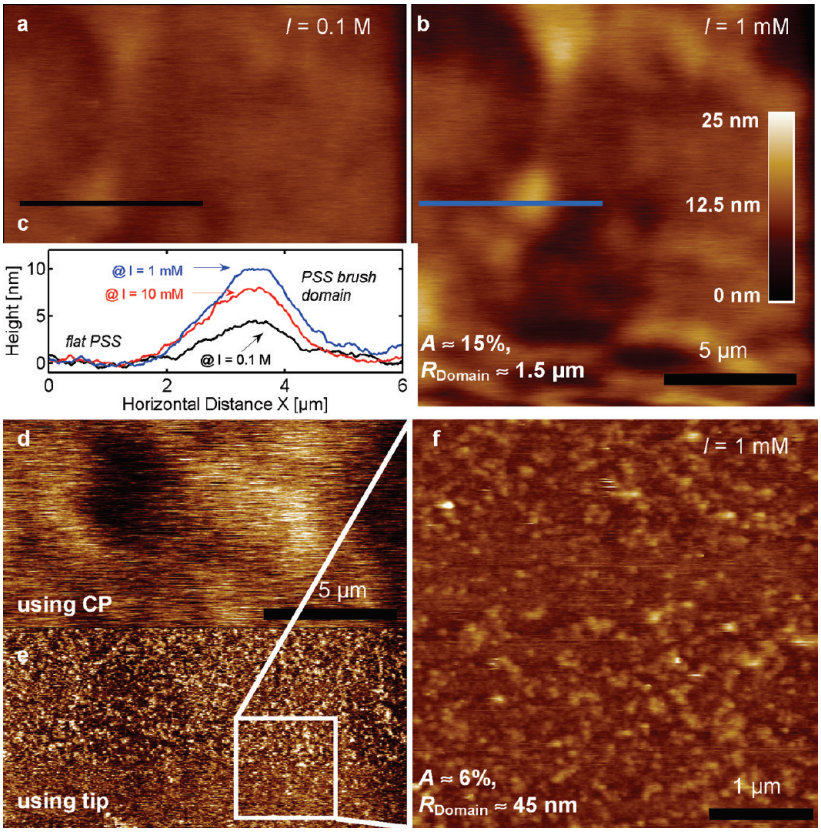

Figure 2. Images of PSS brush domains with $N = 600$ (a−c) and $N = 380$ (d−f). CPTM imaging of PSS ($N = 600$) at (a) $I = 0.1$ M and (b) $I = 1$ mM. The inset (c) gives a cross sections of one brush domain (black and blue lines in a and b, respectively) and shows that the brush domains swell if the surrounding salt concentration I is decreased. In the cross section, we omitted the error bars as the relative error in height determination is below 5% (determined by imaging of rectangular calibration gratings). CPTM imaging of PSS ($N = 380$) with a coarse (d) and a fine lateral resolution ($R \approx 100$ nm, e and f). (d) and (e) are recorded at the same area at $I = 1$ mM. The parameters of the images are scale bar = 5 μm (d, e) and 1 μm (f); z-scale = 5 nm (d, e) and 25 nm (a, b, f). (d) is the same image as Figure 1d, but with smaller z-scale. The layer appears homogeneous only when imaged with the large radius of the CP (d), whereas small islands (brush domains) are visible using a smaller tip radius (e, f). A local increase in area fraction of these domains increases the steric force acting onto the CP. Hence, these areas are less compressed by the CP and appear to be higher on the length scale of the CP; therefore, darker areas in (d) correspond to areas with decreased amount of brush domains in (e) (this can be better seen with the full-sized version of this figure presented in the Supporting Information). (f) Zooms into the marked area of (e) so that the geometry of single brush domains can be resolved.

and to an interaction energy per unit area between a brush and a bare CP

$$\frac{F_{\mathrm{AdG,asymm}}(D)}{2\pi R} = \frac{2k_{\mathrm{B}}TL}{35s^3}\left[7\left(\frac{L}{D}\right)^{5/4} + 5\left(\frac{D}{L}\right)^{7/4} - 12\right] \quad \text{for } D < L \tag{3b}$$

Please note that the AdG theory assumes end-grafted chains, and hence the parameter s also measures the average tail distance. However, as we deal with adsorbed chains, we cannot distinguish between tails and loops, and thus we will summarize both using the term pseudotails[29] and interpret s as average pseudotail distance.

From force measurements performed on flatly adsorbed PSS (i.e., $A = 0$) we know that the electrostatic contribution is independent of N.[27,28,30] Hence, this contribution can be measured independently (cf. with PSS layers adsorbed from salt free solution) and is therefore known in the force profiles eqs 1a and 1b. Furthermore, the parameter A (the area fraction of the 3D brush phase) can be obtained by using CPTM, and hence only two parameters of the steric force, brush thickness L and pseudotail distance s, are unknown in the force profiles eqs 1a and 1b.

For $N = 1800$ the symmetric and asymmetric force profiles are discussed in detail in ref 10 and are completely described by the AdG theory. Qualitatively, the same force is found for $N = 6800$ (cf. Figure 3a), which is consistent with $A = 100\%$ obtained by CPTM measurements for both systems. However, if we compare symmetric with asymmetric measurements for $N = 6800$, we observe no change in the force profiles; i.e., the force profiles of both cases completely match. This property is currently not understood and under investigation in another work.[26] There we observe (by changing the approach velocity of the CP) that the force profile is a superposition of F_{AdG} with an unusual strong hydrodynamic drag force, caused by abnormal high viscosities. Hence, for $N = 6800$ we assume that (due to these deviations from the usual behavior of the PSS brushes) we measure only the asymmetric steric contribution (even in the symmetric case) and neglect any effects caused by symmetric steric contributions.

For $N = 840$ (cf. Figure S2 in the Supporting Information) and $N = 380$ (cf. Figure 3b,c) we find the same qualitative features as for $N = 1800$. However, CPTM shows a surface coverage of ~60% ($N = 840$, Figure 1c) and 6% ($N = 380$, Figure 2f) of the brush phase, and hence one expects a noticeable electrostatic contribution within the force profile. Yet the steric contribution exceeds the electrostatic one by at least 1 order of magnitude and dominates the force profile even at low I (cf. Figure 3b).

Therefore, for $A \ll 100\%$ eqs 1a and 1b can be well approximated by

$$F(D) = F_{\mathrm{DL,asymm}}(D) + AF_{\mathrm{AdG,asymm}}(D) \tag{4a}$$

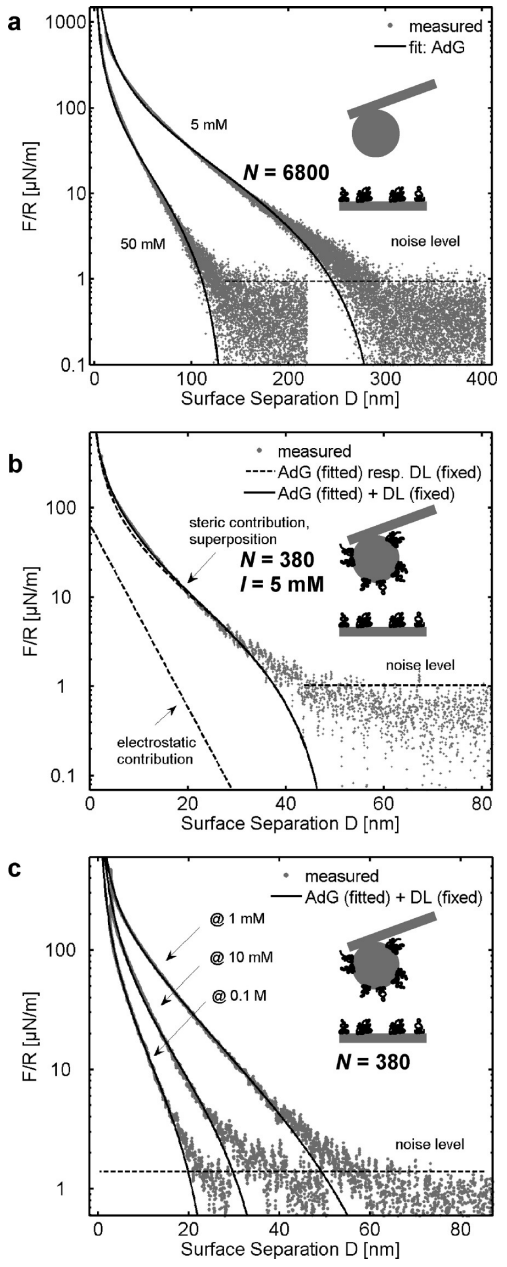

Figure 3. Force profiles between adsorbed PSS layers: (a) $N = 6800$, (b, c) $N = 380$; points: measured profile; lines: fit to the indicated model. The force profiles are well described by the AdG theory, and the steric force exceeds the electrostatic one (measured independently, therefore fixed in the fits) by at least 1 order of magnitude even at low I (cf. dashed line in (b)).

and

$$F(D) = F_{\mathrm{DL,\,symm}}(D) + 2AF_{\mathrm{AdG,\,asymm}}(D) \qquad (4b)$$

Representative fits of eq 4b for $N = 380$ are given in Figure 3c and show that the force profiles are well described by the theory. Summarizing, we can state that the merit of eqs 1 and 4 is not the consideration of the electrostatic force (which is essential for adsorption from $I_{\mathrm{Ads}} < 1$ M NaCl; cf. ref 26) but the proper renormalization of the magnitude of the steric force.

Scaling Laws

In refs 9 and 10 we demonstrated that the brush phase shows properties of neutral brushes and salted polyelectrolyte brushes.

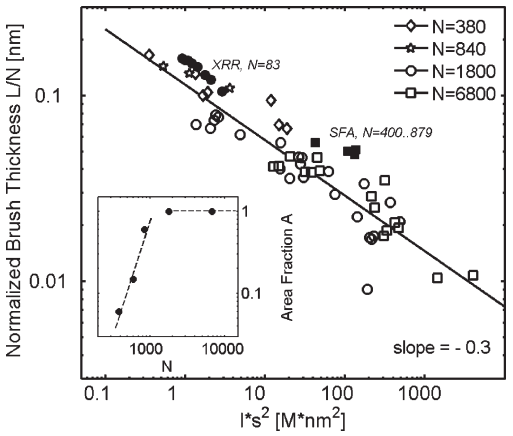

Figure 4. Normalization of the brush thickness L (open symbols obtained from fits to the force profiles of adsorbed PSS, cf. Figure 3) according to the scaling law (eq 5) reduces all data to one master curve (I denotes the surrounding salt concentration and s the average tail distance). Furthermore, our master curve (derived from adsorbed polyelectrolytes) is consistent with parameters obtained by different experimental techniques (i.e., X-ray reflectivity (XRR) by Ahrens et al.[33] and surfaces forces apparatus (SFA) by Li et al.[34]) performed on real end-grafted PSS brushes (full symbols). Obviously, our adsorbed PSS brushes physically behave like end-grafted PSS brushes. The inset shows the 3D area fraction A as a function of the degree of polymerization N (the dashed line corresponds to $A \propto N^{2.5}$). For $N >$ 1100 full surface coverage of the brush phase is obtained.

The neutral properties are the validity of the AdG force law and the absence of electrostatic forces created by the brush. The neutralization by counterion incorporation is a property quite unique to polyelectrolyte brushes.[13] There polyelectrolytes are grafted at one end to the surface whereas the distance between adjacent grafting points s is similar to or smaller than twice the radius of gyration R_g.[8,27,31,32] In this case a chain−chain repulsion (caused by the osmotic pressure of incorporated counterions[31] or excluded volume effects[8]) compels the chains to protrude into solution leading to a PE layer of brush thickness L. The brush thickness can be obtained by calculating the equilibrium between a stretching force (caused by osmotic or excluded volume effects and leading to an extension of the chain) and an entropic elastic restoring force (opposing any chain stretching). These calculations lead to the power/scaling law of the brush thickness L[31,32]

$$L \propto N(Is^2)^{-1/3} \qquad (5)$$

Figure 4 shows the parameters (after fit of eqs 1a and 1b to the measured force profiles for $N = 380-6800$, open symbols) after normalization according to eq 5. Obviously, L scales with -0.3 with respect to Is^2 (a behavior already shown for homogeneous brush layers prepared by adsorption[9,10]) and after normalization by N all data points fall together onto the same master curve. Both facts indicate that the brush phase really behaves like an end-grafted PSS brush. However, if grafting and adsorption lead to the same phase, the data points of Figure 4 should collapse onto the same master curve regardless of how the parameters were obtained. Therefore, we added data obtained by other experimental techniques (Figure 4, solid symbols) performed on real end-grafted PSS brushes: the measurements of Ahrens et al.[33] (X-ray reflectometry (XRR) measurements on PEE−PSS brushes at the air−water interface, grafting density set by a Langmuir trough) and Li et al.[34] (surface forces apparatus (SFA) measurements on PtBS−PSS brushes at the solid−water interface, grafting density set by a Langmuir−Blodgett transfer of an anchor onto mica) whose data points match very well onto the master curve of Figure 4. This shows that it makes physically

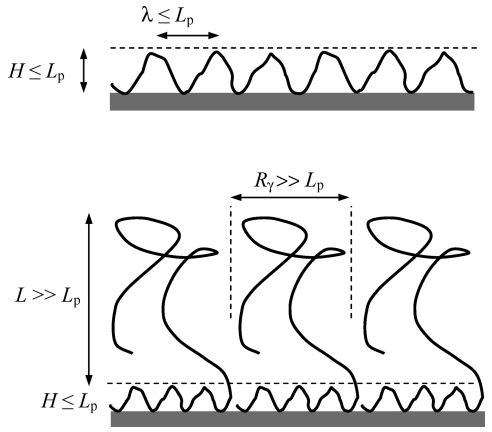

Figure 5. Odijk[35] (top) introduced the length scale λ to describe the behavior of a wormlike chain (WLC) with contour length L_C and persistence length L_p, which is confined within a layer of thickness H. For $L_C > \lambda$, the confined polymer is described as sequence of rigid links with length λ. Netz et al.[25] used these considerations and showed that the polymer is adsorbed if the attractive force (driving the adsorption) equals the osmotic force (caused by reduction in free energy due to confinement). As both forces scale linearly with the monomer count, no dependence on the chain length is observed (top). However, within H it makes no difference if the whole surface is covered by chains adsorbed flatly (top) or coiled (bottom), if the amount of adsorbed monomers is the same. But the adsorption of coiled chains increases the entropy of the system (as the conformational freedom of the system is increased), which is therefore a more preferred state than flat adsorption and leads to a polyelectrolyte brush with brush thickness L. To derive the scaling of the fraction γ of monomers per chain which are adsorbed onto the surface, we compare the gain in entropy (due to increased freedom) with the loss caused by the confinement within a tube of radius R_γ.

no difference if the brush phase was adsorbed (as in our case) or was end-grafted onto an interface. This is a surprising result as on the one hand all monomers of a PSS chain have the same affinity to attach onto the surface. But on the other hand, they create the same structures as if only the end-monomers would be able to adsorb to the surface.

However, the adsorbed brushes appear to be a bit shorter than the end-grafted brushes, indicating that a fraction of each chain is adsorbed onto the substrate. To explain this behavior theoretically, we have to calculate a mixture of flat and coiled adsorption. For flat adsorption we use the theories of Netz et al.[25] and Odijk.[35] Odijk calculated the statistics of a wormlike chain (WLC) of contour length L_C and persistence length L_p, which is confined in a tube of diameter H (cf. Figure 5, top). He introduces a new length scale, the deflection length $\lambda \propto H^{2/3}L_p^{1/3}$ and shows that for $L_C \gg \lambda$ the chain can be regarded as sequence of rigid links, each of length λ. Furthermore, he showed that for $L_C > L_p \geq \lambda$ the free energy increases due to the confinement by

$$\frac{\Delta F_{\text{Odijk}}}{k_B T} \propto \frac{L_C}{\lambda} \ln \frac{L_p}{\lambda} \tag{6}$$

with respect to the unperturbed chain. This equation can be used for our system, as $L_C \geq 100$ nm, $L_p \approx 1.2$ nm,[10] and $L_p \geq H$ (i.e., flat adsorption, which leads to $L_p \geq \lambda$). Netz et al.[25] used eq 6 to calculate an osmotic force acting on the chain due to confinement and showed that adsorption of the polyelectrolyte is possible if this osmotic force is balanced by an (attractive) electrostatic force. The balancing leads to an equilibrium thickness H of the polyelectrolyte layer. Surprisingly, both forces scale linearly with the contour length L_C (cf. eq 6); hence, the scaling laws obtained for H show no dependence on L_C.

However, as long as the whole surface is covered by monomers, it makes energetically no difference within H if the whole chain (cf. Figure 5, top) or only a fraction γ of each polyelectrolyte chain (cf. Figure 5, bottom) is adsorbed onto the surface. As the fraction $(1-\gamma)$ dangles into solution the conformational freedom of the chain is increased, and hence the whole system gains entropy. Therefore, the system should prefer the partial adsorption of chains in order to increase its entropy (with respect to totally flat adsorption, i.e., $\gamma = 1$).

The increase in conformational freedom increases the entropy of one chain and hence reduces the free energy per chain. However, if only a part of the chain is adsorbed, the "unbound" chain fraction will be confined by its neighbors (cf. Figure 5, bottom), and this increases the free energy per chain. Hence, we derive a scaling law for the fraction γ of bound monomers per chain by calculating the minimum in free energy with respect to γ.

We denote the distance between adjacent unbound chains by R_γ and assume that R_γ scales like the radius of gyration of the bound chain fraction, i.e.

$$R_\gamma \propto L_p \left(\frac{a\gamma N}{L_p}\right)^{\nu} \tag{7}$$

Here a denotes the monomer length ($\sim$0.25 nm for PSS) and ν is given by $\nu = 3/(d+2)$ (according to Flory[36]), whereas d denotes the dimensionality of the investigated space. Later we set $d = 2$, as the bound chains form a flat, two-dimensional layer.

The loss in free energy per chain (due to increased entropy) can be calculated as follows: Odjik showed that the change in free energy scales linearly with L_C (cf. eq 6). Hence, if we compare the confinement of the whole chain into the tube of diameter H with the case in which only the fraction γ is confined, the change in free energy reads

$$\frac{\Delta F^+}{k_B T} \propto -(1-\gamma)\frac{L_C}{\lambda} \ln \frac{L_p}{\lambda} \tag{8}$$

However, due to its neighbors the unbound fraction is slightly confined within a tube of diameter R_γ, whereas R_γ is much larger than L_p (cf. eq 7). Therefore, the unbound fraction has the same conformational statistics as a Gaussian coil. Hence, the change in free energy due to neighboring confinement is given by[35]

$$\frac{\Delta F^-}{k_B T} \propto (1-\gamma)\frac{L_p L_C}{R_\gamma^2} \tag{9}$$

Minimizing the sum of eqs 8 and 9 with respect to γ leads to

$$\gamma^{2\nu+1} + \frac{B}{A}\gamma + \frac{2\nu B}{A}(1-\gamma) = 0 \tag{10}$$

with

$$A = -\frac{L_C}{\lambda} \ln \frac{L_p}{\lambda} \quad \text{and} \quad B = \left(\frac{L_p}{L_C}\right)^{2\nu-1}$$

For large $L_C \gg L_p \geq \lambda$, we find $-B/A \ll 1$ and from eq 10 follows $\gamma \ll 1$ (for $\gamma \approx 1$ eq 10 can be written as $\gamma^{2\nu} \sim -B/A \ll 1$ leading to $\gamma \ll 1$, which is a contradiction to the assumption $\gamma \approx 1$). Therefore, eq 10 can be simplified to

$$\gamma^{2\nu+1} \propto -\frac{2\nu B}{A} \tag{11}$$

This leads directly to the scaling laws

$$\gamma \propto N^{-2\nu/(2\nu+1)}, \quad \gamma N \propto N^{1/(2\nu+1)}, \quad \text{and} \quad R_\gamma \propto N^{\nu/(2\nu+1)} \tag{12}$$

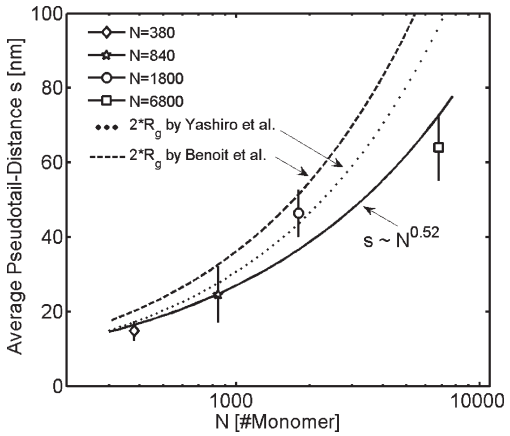

Figure 6. Comparison of the average pseudotail distance s with the radius of gyration R_g of PSS (dotted: experimental values of Yashiro et al.;[37] dashed: theories by Benoit et al., Odjik et al., and Fixman et al.;[38−40] cf. Supporting Information) in dependence on the degree of polymerization N. A scaling law similar to the radius of gyration is obtained. Furthermore, for $N \leq 1800$ the pseudotail distance matches well twice the radius of gyration which indicates that per adsorbed PSS chain at most one brush chain is formed.

which show that this conformation has a stable solution and that the distance R_γ between the unbound chains increases with increasing N, whereas the bound fraction γ decreases with increasing N. Furthermore, in the Supporting Information we calculate the decrease in free energy per unit area Δf which is caused by the additional conformational freedom if the polyelectrolytes adsorb in a coiled conformation instead of a flat one. There we show that $\Delta f \propto -N^{1/(2\nu+1)}$ and hence for $d = 2$ follows $\Delta f \propto -N^{0.4}$. Thus, with increasing N it becomes more favorable for the system to adsorb in a coiled conformation. The same is observed qualitatively, as the area fraction A of the brush domains increases with N (cf. Figure 4, inset) for $N < 1100$ and is constant for $N \geq 1100$.

The theory assumes that the bound monomers are confined within ${R_\gamma}^2$ and that the full surface is covered by monomers, i.e., that there are no holes in the flatly adsorbed layer. If A_0 denotes the area of one monomer, then $\gamma N A_0$ gives the area required by the bound monomers of one chain for close packing and therefore ${R_\gamma}^2$ and $\gamma N A_0$ should be of the same order of magnitude. However, eq 12 shows that ${R_\gamma}^2$ and $\gamma N A_0$ exhibit different scaling laws, but within the investigated range of N (= 380−6800) both terms differ by a factor of less than 1.7, if reasonable values are used (i.e., $A_0 = 45$ Å^2 for PSS,[33] L_p = 1.2 nm and $a = 0.25$ nm[10]). Hence, our assumption of monomer full coverage is self-consistent.

We finish our investigation with the fit of a power law to s (within the adsorbed PSS brush domain). As s should scale like R_γ a test of the developed model is possible. Figure 6 shows $s = s(N)$ (symbols) and the fit of a power law $s \propto N^\alpha$ (solid line). The fit gives an exponent of $\alpha = 0.52$, which is larger than 0.3, the value expected by eq 12 for $d = 2$ and $\nu = 3/4$. This shows that the model holds at least qualitatively and that the calculation of R_γ has to be improved. For example the surface properties (e.g., surface charge) are not considered within the model, and they may have a noticeable influence on R_γ. However, Figure 6 indicates that the pseudotail distance s quantitatively scales similar to twice the radius of gyration (obtained by experiments performed by Yashiro et al.[37] and by applying the theories of Benoit et al., Odjik et al., and Fixman et al.[38−40]) of the whole PSS chain. Hence, the conformation of the PSS chain before adsorption might play an important role too and should be incorporated into a more evolved model.

Conclusion

We show that PSS adsorbs as a two-phase system, the phases differ in PSS conformation (flat vs brush domain) and in surface forces (electrostatic vs steric). Using CP force measurements and CPTM imaging, we are able to fully characterize the properties of the brush phase and to observe the scaling laws for (a) the brush thickness: $L \propto N(Is^2)^{-1/3}$; (b) for the average molecular area: $s^2 \propto N$; and (c) for the brush phase area fraction: $A \propto N^{2.5}$ for $N < 1100$ and $A = 1$ for $N \geq 1100$. Furthermore, the radii of the brush domains vary between 50 nm for $N = 380$ and 1.5 μm for $N = 600$.

We developed a model to show that a stable conformation exists in which the major part of the polyelectrolyte chain extends into the solution, while a fraction $\propto N^{0.4}$ of the monomers is adsorbed onto the substrate. This model explains qualitatively the adsorption behavior of the polyelectrolytes. Additionally, scaling laws for the fraction of bound monomers per chain and for the distance between the unbound chains are derived. We calculate that only for small N most of the monomers are bound to the surface and that longer chains prefer to dangle into solution, a behavior also found in the experiment.

Using these relations, we are now able to build PSS layers with the desired surface properties; cf. the requested magnitude or range of repulsive forces or size of brush domains. Furthermore, Zappone et al.[41] show that absorbed polyelectrolytes can significantly reduce the surface friction coefficient μ. The latter is related to the coiled/brushlike conformation of the chains. Hence, it should be possible to adjust μ by choosing an appropriate value for N, which is a challenge for the future.

Acknowledgment. This work was supported by the Deutsche Forschungsgemeinschaft (TR 24, project B7) and the BMBF (FKZ 03Z2CKI with the ZIK HIKE project) as well as the state of Mecklenburg-Vorpommern and the Stiftung Alfried Krupp Kolleg Greifswald. We thank Burkhard Dünweg for helpful discussions.

Supporting Information Available: Example image showing how the effective curvature radius is obtained; asymmetric force profile for $N = 840$ together with the fits to eq 1a; full-sized version of Figure 2d,e; derivation of the scaling law for the change in free energy per unit area, if the polyelectrolytes adsorb in a coiled instead of a flat conformation; a short overview of the theories of Benoit et al., Odjik et al., and Fixman et al.,[38−40] the equations of which are used to calculate the radius of gyration of PSS. This material is available free of charge via the Internet at http://pubs.acs.org.

References and Notes

(1) Decher, G. *Science* **1997**, *277*, 1232.
(2) Caruso, F.; Caruso, R. A.; Möhwald, H. *Science* **1998**, *282*, 1111.
(3) Yoo, P. J.; Nam, K. T.; Qi, J. F.; Lee, S. K.; Park, J.; Belcher, A. M.; Hammond, P. T. *Nat. Mater.* **2006**, *5*, 234.
(4) Dubois, M.; Schönhoff, M.; Meister, A.; Belloni, L.; Zemb, T.; Möhwald, H. *Phys. Rev. E* **2006**, *74*, 051402.
(5) Hiller, J.; Mendelsohn, J. D.; Rubner, M. F. *Nat. Mater.* **2002**, *1*, 59.
(6) Goodwin, J. *Colloidal Dispersions*; Royal Society of Chemistry: London, 1982.
(7) Farinato, R. S.; Dubin, P. *Colloid-Polymer Interactions: From Fundamentals to Practice*; John Wiley & Sons: New York, 1999.
(8) Pincus, P. *Macromolecules* **1991**, *24*, 2912.
(9) Block, S.; Helm, C. A. *Phys. Rev. E* **2007**, *76*, 030801.
(10) Block, S.; Helm, C. A. *J. Phys. Chem. B* **2008**, *112*, 9318.
(11) de Gennes, P. G. *Adv. Colloid Interface Sci.* **1987**, *5*, 413.
(12) Milner, S. T.; Witten, T. A.; Cates, M. E. *Macromolecules* **1988**, *21*, 2610–2619.
(13) Biesheuvel, P. M. *J. Colloid Interface Sci.* **2004**, *275*, 97–105.
(14) Liberelle, B.; Giasson, S. *Langmuir* **2008**, *24*, 1550–1559.
(15) Claesson, P. M.; Dahlgren, M. A. G.; Eriksson, L. *Colloids Surf., A* **1994**, *93*, 293–303.

(16) Claesson, P. M.; Poptoshev, E.; Blomberg, E.; Dedinaite, A. *Adv. Colloid Interface Sci.* **2005**, *114*, 173.
(17) Berndt, P.; Kurihara, K.; Kunitake, T. *Langmuir* **1992**, *8*, 2486–2490.
(18) Pericet-Camara, R.; Papastavrou, G.; Behrens, S. H.; Helm, C. A.; Borkovec, M. *J. Colloid Interface Sci.* **2006**, *296*, 496–506.
(19) Podgornik, R.; Ličer, M. *Curr. Opin. Colloid Interface Sci.* **2006** *11*, 273–279.
(20) Ducker, W. A.; Senden, T. J.; Pashley, R. M. *Langmuir* **1992**, *8*, 1831–1836.
(21) Meagher, L.; Pashley, R. M. *Langmuir* **1995**, *11*, 4019–4024.
(22) Butt, H. J.; Jaschke, M. *Nanotechnology* **1995**, *6*, 1–7.
(23) Sader, J. E.; Chon, J. W. M.; Mulvaney, P. *Rev. Sci. Instrum.* **1999**, *70*, 3967–3969.
(24) Cleveland, J. P.; Manne, S.; Bocek, D.; Hansma, P. K. *Rev. Sci. Instrum.* **1993**, *64*, 403–405.
(25) Netz, R. R.; Joanny, J. F. *Macromolecules* **1999**, *32*, 9026.
(26) Block, S.; Helm, C. A., to be submitted.
(27) Israelachvili, J. N. *Intermolecular and Surface Forces*; Academic Press: London, 1991.
(28) Butt, H. J.; Cappella, B.; Kappl, M. *Surf. Sci. Rep.* **2005**, *59*, 1–152.
(29) Papastavrou, G.; Kirwan, L. J.; Borkovec, M. *Langmuir* **2006**, *22*, 10880–10884.
(30) Serr, A. Diploma Thesis, University of Geneva, Geneva, Switzerland, **2003**.
(31) Zhulina, E. B.; Birshtein, T. M.; Borisov, O. V. *Macromolecules* **1995**, *28*, 1491–1499.
(32) Naji, A.; Netz, R. R.; Seidel, C. *Eur. Phys. J. E* **2003**, *12*, 223.
(33) Ahrens, H.; Förster, S.; Helm, C. A. *Phys. Rev. Lett.* **1998**, *81*, 4172.
(34) Li, F.; Balastre, M.; Schorr, P.; Argillier, J.-F.; Yang, J.; Mays, J. W.; Tirrell, M. *Langmuir* **2006**, *22*, 4084–4091.
(35) Odijk, T. *Macromolecules* **1983**, *16*, 1340–1344.
(36) de Gennes, P. G. *Scaling Concepts in Polymer Physics*; Cornell University Press: Ithaca, NY, 1979.
(37) Yashiro, J.; Norisuye, T. *J. Polym. Sci., Part B* **2002**, *40*, 2728–2735.
(38) Benoit, H.; Doty, P. *J. Phys. Chem.* **1953**, *57*, 958–963.
(39) Odijk, T.; Houwaart, A. C. *J. Polym. Sci., Polym. Phys. Ed.* **1978**, *16*, 627–639.
(40) Fixman, M.; Skolnick, J. *Macromolecules* **1978**, *11*, 863–867.
(41) Zappone, B.; Ruths, M.; Green, G. W.; Jay, G. D.; Israelachvili, J. N. *Biophys. J.* **2007**, *92*, 1693–1708.